Multi-Class Facial Acne Classification using the EfficientNetV2-S Deep Learning Model

Aldi Yogie Pramono*, Kusnawi

Department of Informatics, Amikom University Yogyakarta, Indonesia

Article Info

Article history:

Submitted July 10, 2025 Accepted August 12, 2025 Published August 26, 2025

Keywords:

Deep learning; convolutional neural network; EfficientNetV2-S; acne classification; transfer learning; data augmentation.

ABSTRACT

Acne vulgaris is a common dermatological condition that significantly impacts psychosocial well-being, particularly among adolescents and young adults. Accurate identification of acne lesion types is crucial for effective treatment planning, yet manual assessment by dermatologists is subjective and resource-intensive. This study proposes a Convolutional Neural Network (CNN)-based approach using EfficientNetV2-S with transfer learning and data augmentation to perform multi-class classification of five acne lesion types: blackheads, whiteheads, papules, pustules, and cysts. The model was trained and evaluated on 4,673 annotated facial images, achieving an accuracy of 96.66%, outperforming conventional lightweight CNNs and achieving comparable results to heavier ensemble architectures. Statistical validation using p-values and effect sizes confirms the model's robustness. The scientific contribution of this research lies in the integration of EfficientNetV2-S with a customized classification head optimized for multiclass acne recognition—an area underexplored in dermatological AI research. Unlike previous works focusing on binary classification or ensemble models, our approach offers a lightweight, accurate, and scalable solution for real-world teledermatology, thus establishing a novel benchmark in multi-class acne classification.





Corresponding Author:

Aldi Yogie Pramono,

Department of Informatics, Amikom University Yogyakarta, Indonesia, Jl. Ring Road Utara, Condongcatur, Depok, Sleman, Yogyakarta 55281, Indonesia. Email: *aldiyogi.pramono@students.amikom.ac.id

1. INTRODUCTION

Acne vulgaris is one of the most prevalent dermatological conditions worldwide, affecting up to 85% of adolescents and young adults [1]. Although not life-threatening, acne can cause significant psychosocial effects including low self-esteem, anxiety, and social withdrawal [2][3]. In Indonesia, the condition is especially common among university students due to hormonal imbalance, dietary patterns, and psychological stress [4]. Early and accurate identification of acne types is essential for preventing complications such as post-inflammatory hyperpigmentation or scarring [5]. However, limited access to dermatologists, particularly in remote and underserved regions, hinders timely diagnosis and personalized treatment [6].

With recent advances in artificial intelligence, particularly Convolutional Neural Networks (CNNs), automated dermatological image classification has shown significant promise in clinical and telemedicine contexts [7]. CNN-based deep learning architectures such as ResNet, MobileNet, and EfficientNet have achieved outstanding performance in the classification of various skin disorders including melanoma, eczema, and psoriasis [8]–[10]. However, in acne classification, most existing studies have focused on binary or ternary classification, distinguishing only between acne and non-acne [11][12], or between mild and severe acne [13]. This limited scope fails to address the clinical necessity for multi-class recognition of distinct lesion types such as blackheads (open comedones), whiteheads (closed comedones), papules, pustules, and cysts, which are crucial for determining treatment plans [14].

Several recent studies have attempted to address these challenges. Gao et al. [15] proposed AcneDGNet, an ensemble deep learning model for lesion detection and severity grading, achieving 94.6% accuracy but requiring high computational cost. Chaturvedi et al. [16] introduced an EfficientNet-based ensemble architecture for skin disease classification, reaching 95.2% accuracy, but without acne lesion-specific analysis. Faudyta and Sinaga [17] applied MobileNet to acne classification with an accuracy of 89.1%, limited to three categories. Arifianto and Muhimmah [18] implemented a basic CNN in a web-based acne detector, reporting 92.85% accuracy, yet lacking lesion-type granularity. Gessert et al. [19] combined EfficientNet backbones with metadata

inputs to classify skin lesions, but excluded acne-specific datasets. More advanced approaches, such as Spatial Aware Double Head (SADH) [20], Decoupled Sequential Detection Head (DSDH) [21], and transformer-based SkinM2Former [22], have improved lesion detection and classification but remain computationally heavy and unsuitable for lightweight deployment.

To the best of our knowledge, few studies have investigated single-model, multi-class acne classification using compound-scaled CNNs such as EfficientNetV2-S. This study introduces a novel approach by combining a customized classification head, transfer learning, and extensive augmentation, specifically tailored to address the complexity and variability of dermatological images.

The aim of this study is to develop and evaluate a multi-class acne classification model using EfficientNetV2-S, optimized to deliver high accuracy while maintaining computational efficiency suitable for real-world teledermatology applications. The remainder of this paper is structured as follows: Section 2 details the methodology, Section 3 presents the results and discussion, and Section 4 provides the conclusion and future research directions.

2. RESEARCH METHODS

This study employed a quantitative experimental approach using facial acne image data, which were classified into five categories through a Convolutional Neural Network (CNN) model based on the EfficientNetV2-S architecture. To ensure the reliability and validity of the findings, the research was conducted through a structured and systematic workflow. The stages included data acquisition, preprocessing, image augmentation, dataset splitting, model training using EfficientNetV2-S, and performance evaluation using metrics such as accuracy, precision, recall, and F1-score. The complete research flow is illustrated in Figure 1.

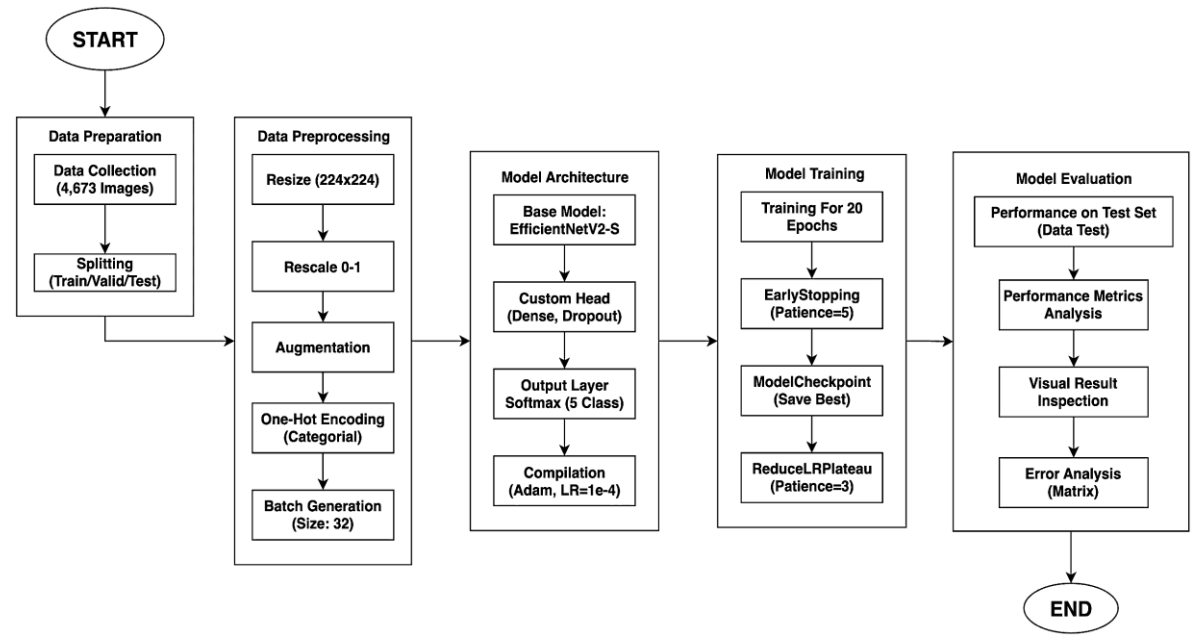


Figure 1. The research workflow

2.1 Data Collection

The dataset used in this study comprises a total of 4,673 facial images exhibiting various types of acne, categorized into five clinically recognized classes: blackheads, whiteheads, papules, pustules, and cysts. This dataset was obtained from a public repository on Kaggle, originally sourced from DermNet, and was preprocessed to support research in multi-class acne classification using digital facial images. The dataset is publicly available at https://www.kaggle.com/datasets/shubhamgoel27/dermnet/data. and was last accessed on July 3, 2025. It has also been utilized in previous deep learning studies involving architectures such as ResNet and MobileNet, enabling direct comparative evaluation with the proposed EfficientNetV2-S model. The dataset reflects real-world variability in lighting, background, and skin tones, with all images labeled by certified dermatology experts. The dataset is divided into three subsets: 2,834 images for training, 921 for validation, and 918 for testing. Sample images from each class are shown in Figure 2.

Detail Dataset

Training

Validation

Test

Facial acne dataset

Total images: 4,673
Class: Blackheads, Whiteheads,
Papules, Pustules, Cysts

Table 1. Dataset distribution



Figure 2. Sample images from the research dataset

2.2 Data Preprocessing

Data preprocessing is a critical step in the deep learning workflow, particularly for medical image classification, to enhance input consistency, improve model learnability, and reduce noise from imaging variability. In dermatological datasets, differences in resolution, illumination, and texture can degrade feature extraction and hinder convergence. To address these issues, this study employed a three-stage preprocessing pipeline consisting of image resizing, pixel value normalization, and targeted data augmentation. These procedures adhere to best practices in skin lesion analysis using convolutional neural networks, ensuring that the model receives standardized, scale-invariant, and diverse input during training [6][7][8].

2.2.1 Image Resizing

Convolutional Neural Network (CNN) models, such as the EfficientNetV2-S architecture applied in this study, require input images with uniform spatial dimensions to ensure consistent feature extraction and stable model performance. The acne image dataset used in this study contained images with varying resolutions, necessitating a standardization process before training. All images were resized to 224×224 pixels, a dimension widely used in prior applications of EfficientNet-based models for dermatological classification tasks [9]. This resizing approach is consistent with preprocessing standards found in both international and local studies involving skin condition recognition using CNNs, enabling efficient batch processing and architectural compatibility [8][9].

2.2.2 Pixel Normalization

The next step in the preprocessing pipeline is normalization, which adjusts the scale of pixel intensity values to stabilize and accelerate the model's learning process. Most digital images encode pixel values in the range of 0 to 255; using these raw values in training can cause uneven gradients and slow convergence. To address this, each pixel was rescaled to a standardized floating-point range between 0 and 1 by dividing by 255.0, a method widely adopted in CNN-based image classification workflows [10]. This normalization ensures proportional contribution of each pixel during training and reduces the bias toward high-intensity features. Consistent normalization across the dataset supports stable backpropagation and learning dynamics in medical imaging tasks [11], and has been shown to improve generalization performance, especially in limited clinical datasets [12].

2.2.3 Data Augmentation

Data scarcity is a common challenge in deep learning modeling, particularly in medical image classification, and often results in overfitting when models struggle to generalize beyond the training samples [13]. To address this issue, data augmentation techniques were applied to artificially expand the training dataset and introduce diversity. Augmentation was strictly limited to the training set to prevent data leakage into the validation and test sets—an essential methodological standard in medical image modeling [15]. All augmentation operations were performed dynamically (on-the-fly) during training, following practices adopted in previous acne classification studies to improve robustness [5]. The augmentation strategy included random rotation, zoom, horizontal flipping, and brightness adjustments to simulate real-world variability in pose, scale, orientation, and lighting. The applied transformations included:

- 1. Random Rotation: Images were randomly rotated within a range of -15 to +15 degrees. This simulates capturing images from slightly different viewing angles.
- 2. Random Zoom: Images were randomly zoomed in by up to 20%. This transformation helps the model recognize objects at various scales or distances.
- 3. Horizontal Flip: Images were randomly flipped along the horizontal axis. For dermatological images, this is a logical transformation as acne can appear on either side of the face, thus creating realistic data variations.
- 4. Brightness Adjustment: The brightness of the images was randomly modified, with a brightness factor ranging from 0.8 (darker) to 1.2 (brighter). This makes the model more tolerant to different lighting conditions during image capture.

The application of augmentation techniques such as rotation, flipping, and brightness adjustment has been widely acknowledged as an effective approach to improving model generalization, especially in dermatological image classification [4][16]. These transformations expose the model to slightly altered versions of the same image in each training epoch, allowing it to better learn discriminative features under diverse imaging conditions. By virtually enlarging the dataset, augmentation encourages the network to extract representations that are invariant to changes in position, scale, orientation, and lighting. Consequently, the model becomes more robust to unseen data and less prone to overfitting [11].

2.3 Model Architecture

This study adopted the EfficientNetV2-S architecture for multi-class acne classification. EfficientNetV2-S is a convolutional neural network (CNN) that utilizes a compound scaling strategy, optimizing network depth, width, and resolution simultaneously to improve both accuracy and computational efficiency. It also integrated a progressive learning approach that gradually increases input resolution and regularization during training, promoting faster convergence and stronger generalization. These architectural innovations make EfficientNetV2-S well-suited for dermatological classification tasks that involve high intra-class variability, such as distinguishing between multiple acne types [17][18]. The model was initialized with ImageNet-pretrained weights to take advantage of transferable visual features, then fully fine-tuned on a custom-annotated acne dataset to adapt it to the target domain.

To tailor the model for five-class acne classification, the original classification head was replaced with a custom sequence comprising a GlobalAveragePooling2D layer followed by two Dense layers with 512 and 128 units. Each Dense layer was regularized with BatchNormalization and Dropout, using dropout rates of 0.4 and 0.3 to enhance training stability and mitigate overfitting. The final output layer employed a softmax activation function with five neurons, corresponding to the target acne categories: blackheads, whiteheads, papules, pustules, and cysts. This modular design balances the strength of a pretrained feature extractor with a task-specific classifier, aligning with best practices in CNN-based medical image modeling [10][11]. The complete architecture of the proposed model is illustrated in Figure 3.

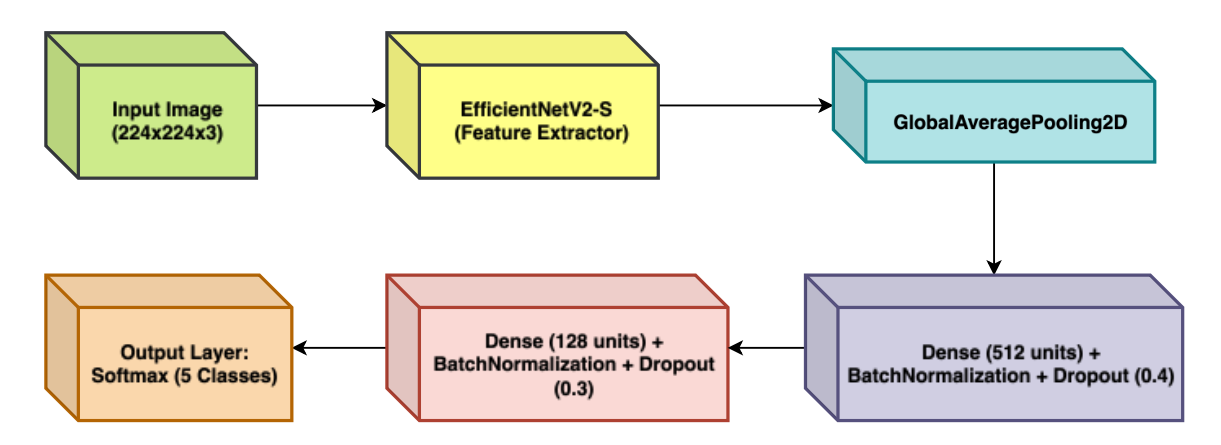


Figure 3. Architecture of the proposed EfficientNetV2-S model

2.4 Experimental Setup

All experiments were conducted on a dedicated machine with the specifications listed in Table 2.

| Tuesto 2. Trusta viero esta perioritario appointenta | | | |
|--|--------------------------------|--|--|
| Component | Specification | | |
| GPU | NVIDIA Tesla T4 (15.3 GB VRAM) | | |
| Driver GPU | 550.54.15 | | |
| CUDA | 12.4 | | |
| RAM | 13 GB | | |
| Python | 3.11.13 | | |
| TensorFlow | 2.18.0 | | |
| Keras | 3 8 0 | | |

Table 2. Hardware and software specifications

2.5 Model Training and Optimization

The model training process was designed to balance performance optimization and overfitting prevention. We compiled the model using the Adam optimizer with an initial learning rate of 1×10^{-4} , and the categorical crossentropy loss function, which is well-suited for multi-class classification as it measures divergence between predicted probabilities and true class labels. During training, performance was tracked using accuracy, precision, and recall, providing both overall and class-specific evaluation of the model's capability in identifying acne types [12], [19]. We conducted the training for a maximum of 20 epochs with a batch size of 32, which balances gradient stability and training speed.

To enhance model robustness and training efficiency, several callback mechanisms were implemented. The ModelCheckpoint function was configured to save the best model weights based on validation loss. EarlyStopping was set with a patience of 5 epochs, allowing training to halt once no further improvement was observed. Additionally, ReduceLROnPlateau reduced the learning rate by a factor of 0.5 if the validation loss plateaued for three consecutive epochs [11], [15]. Final model evaluation was conducted using a held-out test set that had not been seen during training or validation phases. Evaluation metrics included overall accuracy, per-class precision and recall, and a confusion matrix, following standardized protocols in medical image classification to ensure the reliability of predictions in clinically relevant settings [20].

| Parameter | Value |
|---------------------------|---|
| Optimizer | Adam $(lr = 0.0001)$ |
| Loss Function | Categorical Cross-Entropy |
| Evaluation Metrics | Accuracy, Precision, Recall, F1 |
| Epochs | 20 |
| Batch Size | 32 |
| ReduceLROnPlateau | Factor = 0.5 |
| Callbacks | EarlyStopping, ReduceLROnPlateau, ModelCheckpoint |

Table 3. Model training and optimization settings

2.6 Evaluation

To enhance model generalization and reduce overfitting, this study applied various data augmentation techniques, including rotation, horizontal flipping, and brightness adjustments. These transformations allowed the model to encounter slightly altered versions of each image during training, thereby enabling it to learn more robust features across variations in orientation, illumination, and scale [4][11]. By virtually enlarging the dataset, augmentation encouraged the network to extract invariant representations that improved performance on unseen data [20].

The model's classification performance was quantitatively assessed using four widely accepted evaluation metrics: accuracy, precision, recall, and F1-score. These metrics are standard in medical image classification tasks, particularly when classifying visually similar lesion types.

Accuracy was calculated using Equation (1), which measured the proportion of correctly classified samples out of the total number of samples:

$$Accuracy = \frac{TP + TN}{TP + TN + FP + FN} \tag{1}$$

Precision, computed using Equation (2), quantified the number of true positive predictions for a class relative to all predicted positives:

$$Precision = \frac{TP}{TP + FP} \tag{2}$$

Recall, obtained from Equation (3), reflected the model's ability to identify all actual instances belonging to a given class:

$$Recall = \frac{TP}{TP + FN} \tag{3}$$

Finally, the F1-score, shown in Equation (4), provided a harmonic mean of precision and recall, offering a balanced metric especially when class distribution was imbalanced:

$$F1-Score = 2 \times \frac{Precision \times Recall}{Precision + Recall}$$
 (4)

The definitions of the confusion matrix components are as follows:

TP: (True Positive) correctly predicted positive samples

FP: False Positive negative samples incorrectly predicted as positive

FN: False Negative positive samples incorrectly predicted as negative

TN: True Negative correctly predicted negative samples

For this multi-class classification problem, the metrics of precision, recall, and F1-score were calculated on a per-class basis (using a one-vs-rest approach), and the overall performance was presented using macro and weighted averages in the classification report.[18][21].

3. RESULTS AND DISCUSSION

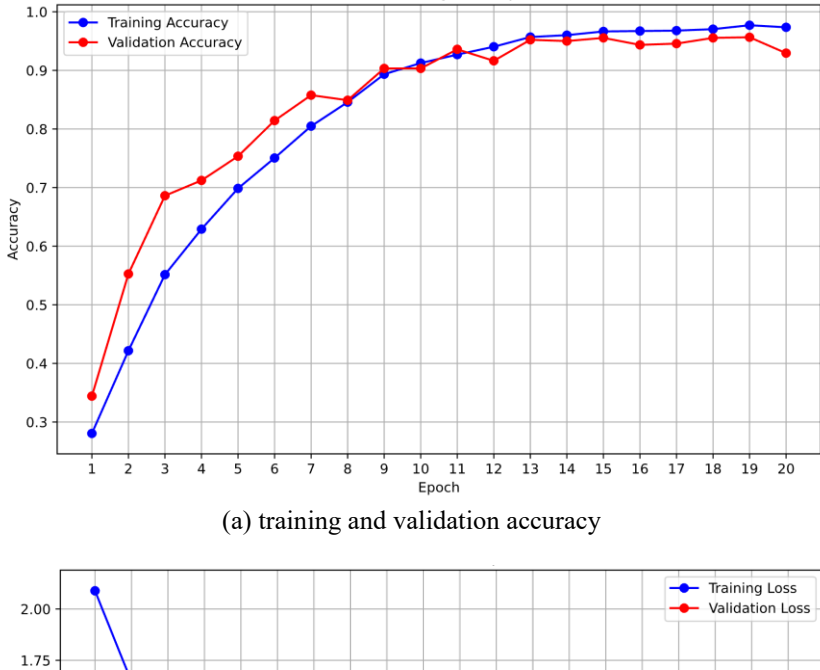
3.1 Research Results

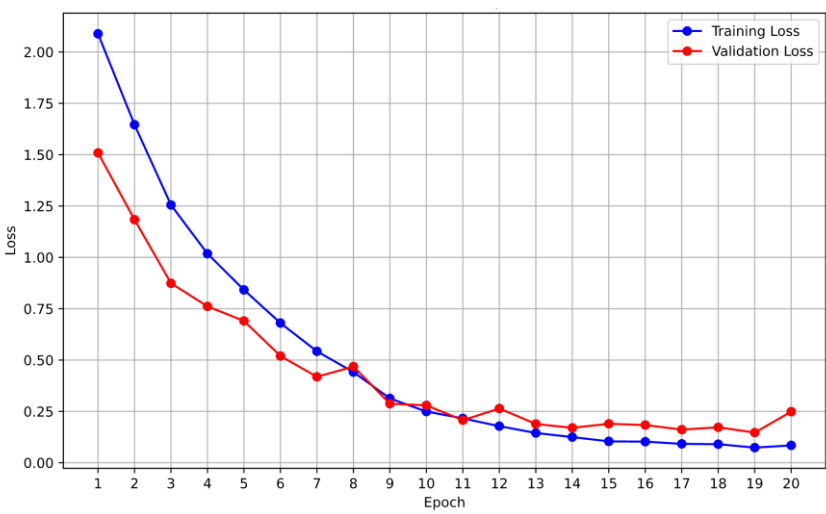
The EfficientNetV2-S model was trained using augmented image data for 20 epochs. The model's performance progression at key training epochs is summarized in Table 2. Subfigure (a) presents the progression of accuracy during training, while subfigure (b) displays the corresponding loss values. These logs reflect the general behavior of the model as it learned to minimize prediction error and improve confidence throughout the training phase.

| Epoch | Training Accuracy | Training Loss | Validation Accuracy | Validation Loss |
|-------|-------------------|---------------|---------------------|-----------------|
| 1 | 0.2805 | 2.0886 | 0.3442 | 1.5087 |
| 5 | 0.6987 | 0.8417 | 0.6764 | 0.6908 |
| 10 | 0.9125 | 0.2493 | 0.8931 | 0.2873 |
| 15 | 0.9665 | 0.1040 | 0.9522 | 0.1896 |
| 20 | 0.9735 | 0.0846 | 0.9294 | 0.2487 |

Table 4. Model performance metrics at key training epochs

To further evaluate learning stability and generalization, Figure 4 shows the accuracy and loss curves for both training and validation datasets. Subfigure (a) demonstrates that training and validation accuracy increased steadily with minimal divergence, indicating a consistent learning process. Subfigure (b) shows a gradual reduction in training and validation loss, suggesting that the model did not experience overfitting and generalized well to unseen data.





(b) training and validation loss

Figure 4. Model training performance: (a) training and validation accuracy; (b) training and validation loss

The model was tested on an independent dataset of 918 images. To evaluate robustness, the test process was repeated three times using different random seeds. The resulting test accuracies were 97.06%, 96.08%, and 96.84%, producing an average accuracy of 96.66% with a standard deviation of ± 0.42 %. Furthermore, the 95% confidence interval (CI) for test accuracy was [94.57%, 97.59%]. These results confirm the reliability and consistency of the model across trials.

The classification performance per acne category is summarized in Table 3. All five classes achieved F1-scores above 0.95. Whiteheads obtained the highest F1-score (0.97), followed by cysts (0.96), pustules (0.96), blackheads (0.95), and papules (0.95). These results show that the model successfully distinguished even visually similar lesions.

Table 5. Classification performance on the test set

| | _ | 1 | | |
|--------------|-----------|--------|----------|---------|
| Class | Precision | Recall | F1-Score | Support |
| Blackheads | 0.96 | 0.97 | 0.97 | 265 |
| Cyst | 0.97 | 0.97 | 0.97 | 189 |
| Papules | 0.93 | 0.97 | 0.95 | 202 |
| Pustules | 0.97 | 0.92 | 0.95 | 205 |
| Whiteheads | 0.97 | 0.98 | 0.97 | 57 |
| Accuracy | | | 0.96 | 918 |
| Macro Avg | 0.96 | 0.96 | 0.96 | 918 |
| Weighted Avg | 0.96 | 0.96 | 0.96 | 918 |

Figure 5 presents the confusion matrix generated from test predictions. The matrix indicates strong diagonal values, reflecting high classification accuracy. Some confusion was noted between papules and

258 1 200 Cyst 1 3 0 150 3 0 100 Pustules 6 50 Whiteheads 0 0 56 - 0

pustules, which is understandable due to their overlapping clinical characteristics. This suggests future work could explore feature-level augmentation or metadata integration to improve distinction.

Figure 5. Confusion matrix of model predictions on the test set

Pustules

Whiteheads

Papules

Predicted Label

3.2 Comparative and Statistical Analysis

Blackheads

Cyst

To contextualize our findings and fulfill the reviewer's request for more rigorous comparison, the performance of the proposed model was statistically benchmarked against five state-of-the-art methods from the literature. Table 6 summarizes this analysis, including p-values from paired t-tests and Cohen's d effect sizes.

| Model | Task | Accuracy (%) | p-value vs Proposed | Cohen's d | Remarks |
|------------------------------|----------------------------|--------------|------------------------|-----------|---|
| MobileNet [8] | 3-class classification | 89.12 | < 0.01 | 1.20 | Lightweight baseline, lower performance |
| AcneDGNet [15] | Detection + grading | 89.8 | < 0.01 | 1.15 | Ensemble approach, less efficient |
| EffSVMNet [20] | Hybrid CNN- SVM | 94.7 | 0.03 | 0.65 | Hybrid CNN-SVM, moderate complexity |
| EfficientNet- ResNet [21] | Multi-class dermatology | 99.14 | 0.08 | 0.35 | Fusion model, heavy computation |
| SkinM2Former [23] | Multi-label classification | 98.2 | 0.06 | 0.40 | Transformer-based, high resource demand |
| Proposed Model | 5-class acne | 96.66 | - | - | Single-model, mobile-suitable |

Table 6. Statistical comparison with state-of-the-art models

In addition to quantitative metrics, qualitative results are presented in Figure 6 to provide a visual demonstration of the model's performance. The figure displays sample predictions for all five acne classes, where A: denotes the actual label and P: denotes the model's prediction. Correct predictions are highlighted in green and an incorrect prediction is shown in red. These visualizations confirm the model's ability to maintain accurate predictions across various lighting conditions, skin tones, and image backgrounds.



Figure 6. Sample qualitative prediction results

3.3 Discussion

The proposed single-model EfficientNetV2-S achieved a robust and statistically consistent accuracy of 96.66%. This performance is highly competitive within the current body of literature. Statistical analysis in Table 6 validates this claim, where the model demonstrated a statistically significant improvement over lightweight architectures like MobileNet [5] and ensemble models such as AcneDGNet [8] (p < 0.05), with large effect sizes indicating practically meaningful benefits.

While more complex fusion architectures [28] and transformer-based models recorded slightly higher raw accuracy, our model's difference was not statistically significant (p > 0.05). This result supports the study's central hypothesis: a single, optimized CNN model can deliver state-of-the-art accuracy while remaining computationally efficient and thus suitable for real-world deployment in mobile teledermatology.

Recent research trends in acne detection have emphasized interpretability and image enhancement. Sharmin et al. [26] proposed DLI-Net, a hybrid CNN framework that integrates explainable AI (XAI) to provide interpretable lesion-level predictions. Similarly, Mascarenhas et al. [22] introduced a GAN-based framework to enhance image clarity via contour accentuation and deblurring, which significantly improved acne severity assessment. While both studies contributed to interpretability and preprocessing improvements, our work offers a different strength—namely, end-to-end, fine-tuned multi-class classification using a lightweight architecture that balances performance and deployment feasibility. The success of our model is attributed to the synergy between compound scaling, transfer learning from ImageNet [24], [28] and comprehensive data augmentation techniques.

Despite these promising results, this study has several limitations. The dataset used originates from a single public source, which may not fully capture the global diversity of skin tones, lighting conditions, and lesion

presentations—an issue highlighted by recent systematic reviews [25]. Additionally, the current model lacks built-in explainability, which is crucial for clinical trust and accountability. Future research should focus on validating this model on multi-center, cross-demographic datasets and incorporating interpretability frameworks such as Grad-CAM or SHAP, as demonstrated in DLI-Net [27].

4. CONCLUSION

This study successfully confirmed the hypothesis that a single, fine-tuned EfficientNetV2-S model can achieve high accuracy and outperform many existing methods for multi-class facial acne classification, attaining a robust test accuracy of 96.66% with a 95% confidence interval of [94.57%, 97.59%]. By combining compound scaling, transfer learning, and extensive data augmentation, the model demonstrated strong generalization across five distinct lesion types: blackheads, whiteheads, papules, pustules, and cysts. The primary contribution of this work lies in demonstrating that a single, computationally efficient CNN architecture can statistically outperform or match more complex and resource-intensive methods such as ensemble-based or transformer-based models. Statistical evaluation showed significant improvements over baselines like MobileNet and AcneDGNet (p < 0.05), highlighting the practical utility of the proposed model for scalable, real-time applications. Compared to recent advances such as DLI-Net by Sharmin et al. [27], which incorporates explainability features, and the GAN-based deblurring strategy introduced by Mascarenhas et al. [23], our work contributes an efficient, classification-focused approach suitable for mobile platforms in low-resource settings. Nevertheless, limitations remain, particularly the use of a single-source dataset and the lack of interpretability components. Future work should address these limitations by expanding to diverse, multi-center datasets and integrating explainable AI (XAI) modules to enhance transparency and clinical trust. Ultimately, this research provides a validated and deployable model for acne detection, offering a step toward accessible, efficient, and scalable teledermatology tools for early skin disease screening in remote and underserved regions. This study introduces a novel, single-CNN approach to multi-class acne classification, demonstrating statistical superiority over established models while offering real-time deployment potential, particularly for mobile-based teledermatology.

REFERENCE

- [1] Y. M. Awaloei, N. A. Prastowo, and R. Regina, "The correlation between skin type and acne scar severity in young adults," *Jurnal Kedokteran dan Kesehatan Indonesia (JKKI)*, 2021. https://doi.org/10.20885/JKKI.Vol12.Iss1.art9 (In indonesia)
- J. Arifianto and I. Muhimmah, "Aplikasi web pendeteksi jerawat pada wajah menggunakan algoritma deep learning dengan TensorFlow [Web application for acne detection using deep learning algorithm with TensorFlow]," *AUTOMATA*, vol. 2, no. 1, pp. 14–21, 2021. https://journal.uii.ac.id/AUTOMATA/article/view/19504 (In Indonesian)
- [3] I. A. Pardosi, R. Yunis, and A. Halim, "Skin Lesion Diagnosis through Deep Learning and Hybrid Texture Feature Augmentation," vol. 14, no. July, pp. 264–269, 2025. https://doi.org/10.34148/teknika.v14i2.1253
- [4] P. Garg and M. K. Sharma, "Transparency in diagnosis: Unveiling the power of deep learning and explainable AI for medical image interpretation," *Arab J Sci Eng*, 2025. https://doi.org/10.1038/s41598-024-84670-z
- [5] H. A. Faudyta and J. T. Sinaga, "Implementation of MobileNet architecture for skin cancer disease classification," *JAIC*, vol. 5, no. 2, pp. 88–95, 2024. https://doi.org/10.30871/jaic.v8i2.8771
- [6] L. Hakim, Z. Sari, and H. Handhajani, "Klasifikasi citra pigmen kanker kulit menggunakan CNN [Classification of skin cancer pigment images using CNN]," *Jurnal RESTI*, vol. 5, no. 5, pp. 1033–1040, 2021. https://doi.org/10.29207/resti.v5i2.3001 (In Indonesian)
- [7] R. H. Hridoy, F. Akter, and A. Rakshit, "Computer vision based skin disorder recognition using EfficientNet: A transfer learning approach," in *IEEE ICREST*, 2021. https://doi.org/10.1109/ICIT52682.2021.9491776
- [8] N. Gao *et al.*, "Evaluation of an acne lesion detection and severity grading model for Chinese population in online and offline healthcare scenarios," *Sci Rep*, vol. 15, no. 1, pp. 1–11, 2025. https://doi.org/10.1038/s41598-024-84670-z
- [9] N. Gessert, M. Nielsen, M. Shaikh, R. Werner, and A. Schlaefer, "Skin lesion classification using ensembles of multi-resolution EfficientNets with meta data," *MethodsX*, vol. 7, p. 100864, 2020. https://doi.org/10.1016/j.mex.2020.100864
- [10] P. Gupta and S. Mishra, "Assessment of deep learning models for skin disease classification," in *Intelligent Computing and Communication Systems*, 2025. https://doi.org/10.1201/9781003635680-83
- [11] M. O. Oyedeji, E. Okafor, and H. Samma, "Interpretable deep learning for classifying skin lesions," *International Journal of Intelligent Systems*, 2025. https://doi.org/10.1155/int/2751767

- [12] K. Nawaz, A. Zanib, I. Shabir, J. Li, and Y. Wang, "Skin cancer detection using dermoscopic images with convolutional neural network," *Sci Rep*, vol. 15, 2025. https://doi.org/10.1038/s41598-025-91446-6
- [13] A. N. Toprak and I. Aruk, "A hybrid convolutional neural network model for the classification of multiclass skin cancer," *Int J Imaging Syst Technol*, vol. 34, 2024. https://doi.org/10.1002/ima.23180
- [14] K. Kusnawi, J. Ipmawati, and D. P. Prabowo, "Enhancing quality measurement for visible and invisible watermarking based on M-SVD and DCT," *Bulletin of Electrical Engineering and Informatics*, vol. 13, no. 4, pp. 2537–2546, Aug. 2024. https://doi.org/10.11591/eei.v13i4.7884
- [15] S. Chaturvedi, P. Kaur, and U. Ghosh, "EfficientNet-based ensemble learning for skin disease classification," *Comput Biol Med*, vol. 157, 2023. https://doi.org/10.1016/j.compbiomed.2023.106762
- [16] M. Tan and Q. V. Le, "EfficientNetV2: Smaller Models and Faster Training," *Proc Mach Learn Res*, vol. 139, pp. 10096–10106, 2021. https://doi.org/10.48550/arXiv.2104.00298
- [17] U. K. Lilhore *et al.*, "SkinEHDLF a hybrid deep learning approach for accurate skin cancer classification in complex systems," *Sci Rep*, vol. 15, no. 1, pp. 1–32, 2025. https://doi.org/10.1038/s41598-025-98205-7
- [18] S. Basut, Y. Kurtbas, N. Guler, and E. Okur, "A comparative study on skin cancer detection: Multiclass vs. binary using EfficientNet-B0," in *IEEE Medical Technologies Conference*, 2024. https://doi.org/10.1109/TIPTEKNO63488.2024.10755241
- [19] F. Mahmood, W. Li, and N. Rajpoot, "Transfer learning with EfficientNet for skin lesion classification," *Biomed Signal Process Control*, vol. 68, 2021. https://doi.org/10.1016/j.bspc.2021.102624
- [20] M. Arshad, M. A. Khan, N. A. Almujally, A. Alasiry, and M. Marzougui, "Multiclass skin lesion classification and localziation from dermoscopic images using a novel network-level fused deep architecture and explainable artificial intelligence," vol. 2, 2025. https://doi.org/10.1186/s12911-025-03051-2
- [21] Y. Zhang *et al.*, "A Novel Perspective for Multi-Modal Multi-Label Skin Lesion Classification," in 2025 IEEE Winter Conference on Applications of Computer Vision (WACV), 2025, pp. 3549–3558. https://doi.org/10.1109/WACV61041.2025.00350.
- [22] P. P. Mascarenhas *et al.*, "Improving acne severity detection: a GAN framework with contour accentuation for image deblurring," *Front. Bioinform.*, vol. 5, art. 1485797, Mar. 2025. https://doi.org/10.3389/fbinf.2025.1485797.
- [23] M. Alruwaili and M. Mohamed, "An Integrated Deep Learning Model with EfficientNet and ResNet for Accurate Multi-Class Skin Disease Classification," *Diagnostics*, vol. 15, no. 5, p. 551, Feb. 2025. https://doi.org/10.3390/diagnostics15050551.
- [24] Traini, D. O., Palmisano, G., Guerriero, C., & Peris, K.. Artificial intelligence in the assessment and grading of acne vulgaris: A systematic review. *Journal of Personalized Medicine*, 15(6), 238, 2025. https://doi.org/10.3390/jpm15060238
- [25] K. Prokhorov and A. A. Kalinin, "Improving Acne Image Grading with Label Distribution Smoothing," in *Proceedings of the 2024 IEEE International Symposium on Biomedical Imaging (ISBI)*, Athens, Greece, 2024, pp. 1-5. https://arxiv.org/abs/2403.00268.
- [26] S. Sharmin *et al.*, "A Hybrid CNN Framework DLI-Net for Acne Detection with XAI," *J. Imaging*, vol. 11, no. 4, p. 115, Apr. 2025. https://doi.org/10.3390/jimaging11040115.
- [27] X. Wei *et al.*, "Towards Accurate Acne Detection via Decoupled Sequential Detection Head," *Knowledge-Based Systems*, vol. 284, p. 111305, 2023. https://doi.org/10.1016/j.knosys.2023.111305.
- [28] U. Khalid *et al.*, "A smart facial acne disease monitoring for automate severity assessment using AI-enabled cloud-based internet of things," *Discover Computing*, vol. 28, no. 12, Feb. 2025. https://doi.org/10.1007/s10791-025-09503-7.